Polymer 50 (2009) 305–316

Contents lists available at ScienceDirect

Polymer

journal homepage: www.elsevier.com/locate/polymer

Modeling the structure of a polydisperse polymer brush

Wiebe M. de Vos*, Frans A.M. Leermakers

Laboratory of Physical Chemistry and Colloid Science, Wageningen University, Dreijenplein 6, 6703 HB Wageningen, The Netherlands

ARTICLE INFO

Article history:
Received 24 July 2008
Received in revised form
15 October 2008
Accepted 21 October 2008
Available online 26 October 2008

Keywords:
Polymer Brush
Polydispersity
Self-consistent field theory

ABSTRACT

Numerical self-consistent field theory is used to study the structural characteristics of a polydisperse polymer brush. We consider the relevant case of a Schulz–Zimm distribution and find that even a small degree of polydispersity completely destroys the parabolic density profile. The first moment (average height) of the brush increases with polydispersity, while the average stretching in the brush decreases. The density profiles of separate chain length fractions in a single polydisperse brush are also strongly influenced by polydispersity. Short chains are found to be compressed close to the grafting interface, whereas longer chains have a characteristic flower-like distribution. These longer chains stretch strongly (stem) when surrounded by smaller chains and decrease their stretching (crown) when only surrounded by longer chains. In line with approximate analytical models, our numerical exact results show that the polymer chains in the brush have localized end-point positions (no fluctuations) in strong contrast to the anomalously large fluctuations in the end-point positions of the homodisperse brush. Despite these effects, the scaling of average height with grafting density and number average chain length is unaffected by polydispersity. Many results that we have presented can be understood qualitatively from the bidisperse brush.

1. Introduction

Polymer brushes, densely packed arrays of polymer chains end-attached to an interface, have been the subject of many experimental and theoretical investigations in the past 30 years [1–3]. There are however significant differences between the theoretical and experimental investigations of polymer brushes. One is that most theories assume strong stretching of the polymer chains in the brush, while it is hard for an experimentalist to achieve densities high enough for this strong stretching [4]. Another significant difference is the polydispersity. While it is practically impossible for an experimentalist to produce a perfectly homodisperse polymer brush, almost no theoretical work has been done on the effect of polydispersity with a realistic size distribution.

Polydispersity in polymer brushes has already received some attention from the modeling point of view. In particular there has been some interest in the modeling of the simplest form of polydispersity, a brush containing two chemically identical fractions with polymers of different length. Approximate analytical self-consistent field theory has been developed by Milner, Witten and Cates (MWC) [5] and by Birshtein et al. [6]. In these analytical theories one typically assumes the complete segregation of end points of the long and short polymer fractions. Although it is known that end points do segregate, such assumption should be the outcome of the analysis rather than the input. Another assumption is that the local stretching of a chain is determined only by the local chain density. A key result of this approach is the prediction that the density profile of the short fraction is unaffected by length and content of long chains (at fixed grafting density). Both sets of authors also predict that the mixing of long and short chains increases the entropy of a brush. Comparing their models to Monte Carlo (MC) simulations revealed differences, mainly attributed to some overlap of end points of the long and short fractions [7]. For a uniform distribution of chain lengths as described by MWC the calculated density profile compares well to MC simulations.

To our knowledge there exists just one analytical SCF study wherein no *a priori* assumption is made on the position of end points. Klushin and Skvortsov [8] used an ingenious trick to extract information for a polydisperse brush from the known properties of a homodisperse one. The start of their analysis is the analytical SCF theory of the homodisperse brush, i.e. the brush described by the strong stretching approximation. For very long chains we know that the results are accurate and that for finite chain length there are shortcomings due to fluctuations of chain conformations beyond those accounted for in the most-likely trajectories. The second step in the analysis is to assign a plane inside the brush and analyze the lengths of all chain parts that reside outside this plane. This population of chain parts consists of short ones that are less

* Corresponding author. Tel.: +31 317 481491.
E-mail address: wiebe.devos@wur.nl (W.M. de Vos).

0032-3861/$ – see front matter © 2008 Elsevier Ltd. All rights reserved.
doi:10.1016/j.polymer.2008.10.025

strongly stretched and have their free ends not far from the assigned plane, and longer ones that are more stretched because the free chain end is further from the assigned plane. As a result there exists a full set of lengths with corresponding grafting densities (as evaluated from this reference plane). The third step is to freeze the plane and take this plane as the grafting surface of the polydisperse distribution of chain lengths found in step two. All properties of this polydisperse brush are known. The overall profile, for example, is parabolic and the local stretching is the same as that in the homodisperse reference brush. The resulting chain length distributions consist of many long chains and few shorter chains and thus, these authors could consider only very small degrees of polydispersities. One of the main predictions is that the end-point fluctuations decrease with increasing polydispersity. They also predict for low polydispersities, independent of the chain length distribution, that the height H of a polymer brush increases with polydispersity, i.e. increases with the weight average molar mass over the number average mass (M_w/M_n), as $\delta H = (M_w/M_n - 1)^{1/2}$. Currently, it is unknown whether this law also applies to more realistic polymer length distributions.

Dan and Tirrell [9] have investigated bidisperse brushes using a numerical SCF (nSCF) model very similar to the model used below. In this numerical approach these authors also could account for the fact that the end-point distributions of the long and short chains overlap to some extent. They performed a thorough study varying the fraction and the difference in length of the long and short polymer end-grafted chains. They found that the longer chains stretch significantly more than the shorter ones near the grafting interface and that the density profile of the short chain is influenced by the length and content of long ones. Indeed, this complication is the reason for the extremely low attention of the polymer brush community for the effects of polydispersity. There is a lack of rigorous approaches to this problem. As a result the current situation is rather unsatisfactory. On the one hand polydispersity is an inherent aspect of any experimental system but the modeling community ignores this aspect as much as possible.

Results from neutron reflection have been compared extensively to nSCF models (using predictions for homodisperse polymers in a number of papers [10,11]) and are found to compare well. At this stage we might wonder why such good correspondence was found. One possible reason for this is that a small polydispersity does not destroy the expected scaling behavior of the height with the average chain length and overall grafting density. Much less is known about brushes with deliberate polydispersity. Kritikos investigated, using the neutron reflection technique a tridisperse system and analyzed the results with nSCF and concluded that there exists a segregation in height and stronger stretching for a long chain surrounded by smaller chains, very similar as for a bidisperse brush [12].

As stated above, almost no theoretical work has been done on the effect of a realistic form of polydispersity on a polymer brush. We found only a single work by Terzis et al. [13] who investigated using an SCF model a polymer brush with a realistic size distribution in contact with a polymer melt of chemically equivalent chains. They show that increasing the polydispersity leads to improved miscibility between the brush and the polymer melt. This is a strong indication that polydispersity can have very pronounced effects on the properties of a polymer brush.

In this paper we investigate the effect of polydispersity on a polymer brush in a good solvent, again using an nSCF model. For the polydispersity we use the Schulz–Zimm distribution, a realistic size distribution often used to describe polymer polydispersities. We investigate the effect on the overall brush density profiles and on the structure of a polydisperse brush by studying the density profiles and end-point distributions of single fractions in the polydisperse brush. We also present a very simple analytical model for polydispersity based on the Alexander and De Gennes box model.

2. Theory

2.1. Numerical self-consistent field theory

There exists a strong analogy between the path followed by a Brownian particle and the conformation of a (Gaussian) polymer chain. As a result, there exists a diffusion-like equation to describe such a polymer system. Polymers with excluded volume have perturbed (non-Gaussian) conformations and, on a mean-field level, one can treat this problem by considering a diffusion problem in an external potential field. Then, in self-consistent field theory the potential is chosen to be a function of the volume fraction (dimensionless concentration) of polymer and the potential assumes the property of self-consistency. This scheme was invented by Edwards and the corresponding diffusion equation carries his name. The Edwards diffusion equation needs to be solved in a particular geometry by specifying the initial and boundary conditions [14]. Exact analytical solutions, especially for situations that the polymer molecules are strongly interacting are not available, only analytical approximations exist.

Numerical solutions for the case that polymers are end-grafted can be generated only after choices have been made about the discretisation scheme. Here we follow the approach of Scheutjens and Fleer (SF-SCF) [15], wherein the polymer segment size matches the cell size of the spatial coordinates. In this scheme the conformations of the polymers are described by freely jointed chains, which have the property of finite extensibility. This means that no polymer chain that is attached with the first segment to the wall can have its Nth segment more than N lattice sites away from the surface. The discrete version of the Edwards equation reduces to a set of recurrence equations, also known as propagators.

The propagator formalism can be set up extremely efficient such that the number of computations for the whole set of polymer chains is comparable to the evaluation of the volume fraction of the largest chain in the distribution [16]. As such an efficient scheme has not been discussed in the literature for end-grafted chains, we discuss the details of this in Appendix 1. Apart from this technical issue, there is no additional difficulty as compared to the evaluation of properties of homodisperse brushes. Details of this [10,17] can easily be found in the literature and we do not go into more detail here, apart from mentioning that the inter-chain excluded-volume effects are accounted for by the segment potentials, which in the absence of specific interactions are given by $u(z) = -\ln(1-\varphi(z))$, where z is the distance in units of lattice sites away from the grafting surface, and φ is the volume fraction of segments. For not too high volume fractions and good solvents we thus find $u(z) \approx \varphi(z)$.

For homodisperse brushes it can be shown that the potentials, $u(z)$, are essentially parabolic ($u(z) = \alpha(A - Bz^2)$) and thus that the volume fraction profiles are parabolic. In polydisperse cases polymers with different molecular weights are present. This complicates the issue and strong deviations from this parabolic law are expected. In summary, the key input that is needed for the execution of the SF-SCF method is to feed the formalism with a distribution of chain lengths (degrees of polymerization). As the chain length must remain finite one also has to define the upper limit of the size distribution by choosing an appropriate maximum chain length. In Section 2.3 we will go into more details.

2.2. Polymer length distribution

A function commonly used to represent polymer molecular weight distributions is the so-called Schulz–Zimm distribution [18,19]:

$$P(x,N_i) = \frac{x^{x+1}}{\Gamma(x+1)}\frac{N_i^{x-1}}{N_n^x}\exp\left(-\frac{xN_i}{N_n}\right) \quad (1)$$

In which $P(N_i)$ is the probability of chains with degree of polymerization N_i, N_n is the number average degree of polymerization and x defines the broadness of the distribution. $\Gamma(x+1)$ is the so-called gamma function which for integer values of x is equal to $x!$. A nice feature of this distribution is that the parameter x is directly related to the polydispersity:

$$\frac{M_w}{M_n} = \frac{N_w}{N_n} = \frac{x+1}{x} \quad (2)$$

In Fig. 1 we show the Schulz–Zimm distribution for a number of polydispersities used throughout this paper. As can be seen the distribution is almost symmetrical at low values of the polydispersities, but with increasing polydispersities the distribution shifts to a larger frequency of small chains. At the highest polydispersity given in Fig. 1 ($M_w/M_n = 2$) the maximum in the distribution occurs at the lowest chain lengths and there is a continuous decrease of the occurrence of chains with increasing chain length. This implies that the number of molecules of length $N_i = 1$ is in fact larger than any particular polymer length.

Here we follow the strategy presented in Appendix 1 to number the chains by an index i and assume that chain i has a length $N = i$ so that we can interchange notation. The overall grafting density σ is defined as the number of chains per unit area. The grafting density per chain length therefore is given by $\sigma_i = P(x,N_i)\sigma$ and the largest chains are given by N_l.

2.3. Parameter settings

When varying the polydispersity, we have implemented that the number average degree of polymerization, the overall grafting density and the overall mass are always preserved. Unless specified otherwise we have considered the Schulz–Zimm distribution with a maximum chain length of $N_l = 1000$. All interaction parameters are taken as zero so that the polymer segments have no specific affinity with the surface and the solvent is athermal. In some of the calculations we consider a special distribution where only two chain lengths are used (bidisperse brush). In that case the chain lengths and the grafting densities are specified separately.

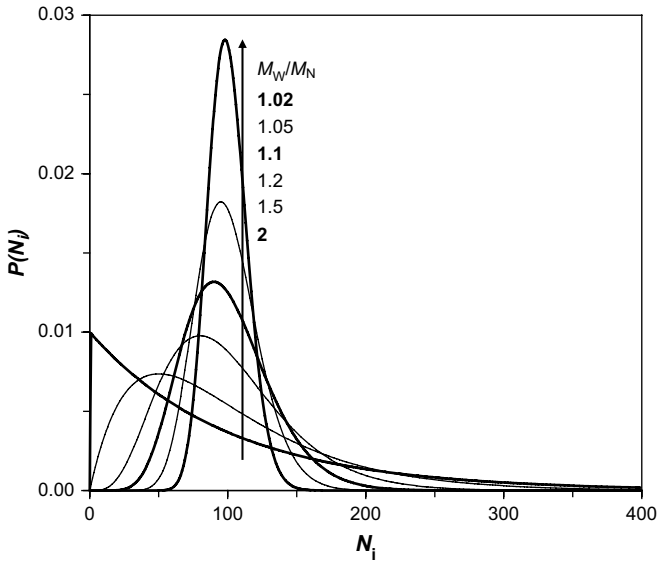

Fig. 1. Schulz–Zimm distribution for different polydispersities, the probability for length N_i, $P(N_i)$ is plotted (see Eq. (1)).

In the lattice model one typically uses dimensionless quantities, i.e. concentrations are expressed in volume fractions and the distances are expressed in lattice units. For conversion to real concentrations and actual distances it is necessary to choose a segment length (equal to the lattice spacing). A reasonable value for this parameter is $b = 0.5$ nm. The chains are grafted to a solid surface and the solvent is monomeric. The system volume is chosen large enough so that the outer boundary is well above the brush height H.

3. Results

3.1. Bidisperse brushes

The exact solutions of the SCF equations for the general case of a polydisperse mixture are not available and therefore we now turn our attention to the numerical SCF method of Scheutjens and Fleer. The simplest form of polydispersity is a mixture of two polymer fractions with different lengths and equal grafting densities. This system has already been addressed by a number of studies [5,6,9,12,20]. We take a somewhat different approach than already performed studies, instead of changing the length (or grafting density) of one polymer fraction while keeping the other chain length fraction constant we change both chain fractions, which have identical grafting densities, simultaneously. As one chain length fraction becomes longer and the other chain length fraction becomes equally shorter, the average chain length, total mass and grafting density are thus conserved. This has the advantage that all changes in the overall brush density profile can be attributed completely to polydispersity and not to any other change in parameters. This for instance allows us to, for the first time, investigate the effect of bidispersity on the average stretching of the chains in the brush. Another difference with earlier studies is that we not only investigate cases were there is a large difference between the long chain fraction and the short chain fraction, but also cases were the chain length fractions differ only a few monomers in length. We present our results in Fig. 2 which shows the change in the overall volume fraction profiles of such bidisperse brush upon an increasing disparity between the lengths of the two fractions. In this graph we conserved both the total grafting density and the total mass.

In Fig. 2a we demonstrate how the increasing differences between the two polymer fractions influence the overall brush profile. Indeed, for small differences, the profile does not deviate much from that of a parabolic profile of a monodisperse brush. For larger differences, however, the profile resembles that of two parabola one on top of the other, and the height of the brush as judged from the fact that the overall volume fraction extends to larger z-values increases with increasing chain length difference.

In Fig. 2b we show the volume fraction profiles of the two separate fractions as well. In this graph the profile of the smaller chain is dotted, and the profile for the longer chain is the solid line. As the grafted amount is fixed $\sigma_1 N_1 + \sigma_2 N_2 = \sigma(N_1 + N_2)/2 = 10$, the integral of the two profiles is conserved. Important is that even though the total brush density is not influenced much by small differences, the separate contributions are strongly affected by small length differences. A length difference of 10 monomers ($N_1 = 95$ and $N_2 = 105$) is enough to reduce the volume fraction of the long polymer close to the grafting interface by 25%. The concentration of the short fraction increases by a similar amount. The shape of the density profile of the short polymer resembles a parabolic profile in all cases. The profile of the long chains shows a flat region when surrounded by much small chains and after that an increase and then a parabolic-like decrease. This profile indicates a strong stretching of the longer chains when surrounded by much of the smaller chains. Such result was already shown by Dan

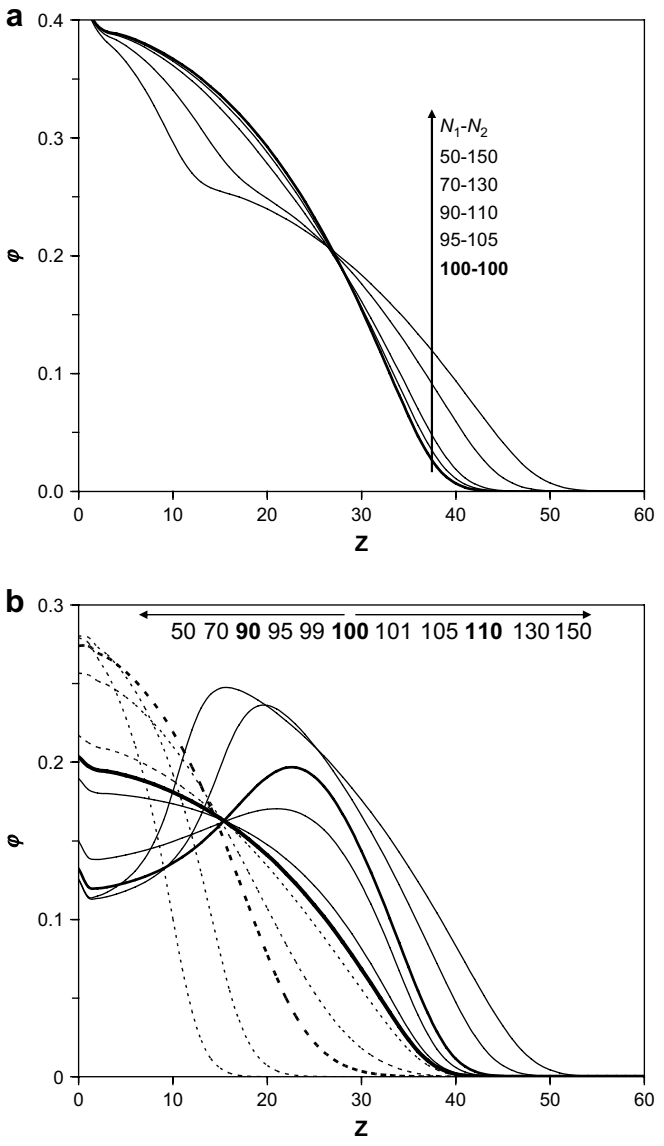

Fig. 2. (a) Overall volume fraction profiles of a brush containing two fractions, one fraction increases in length and the other decreases an equal amount. $\sigma_{long} = \sigma_{short} = 0.05$. $N_n = 100$. (b) The corresponding volume fraction profiles of the separate fractions. The short ones are dotted and the long ones are drawn by a continuous line.

and Tirrell [9]. This is however a rather qualitative result. To exactly determine how much more the long chain stretches compared to the short chain at a certain position in the brush one can calculate the local stretching as a function of z. Results of such a calculation are given in Appendix 2 that confirm the qualitative prediction.

The end-point distribution $\varphi_e(z)$ (see Appendix 1 Eq. (A4)) plays an important role in polymer brush theory (see also Appendix 2, Eq. (A7)). The interesting issue here is that for the homopolymer brush the end points are distributed throughout the brush. Indeed, the end-point distribution grows approximately linearly with the distance from the grafting surface and only at the periphery of the brush the end-point distribution suddenly drops to zero. Such wide distribution of the end points manifests anomalously large fluctuations present in the homopolymer brush. The end-point fluctuations are proportional to the chain length. With this in mind it is appropriate to investigate how the end points are distributed in the polydisperse brush, and we will begin this investigation by looking at these distributions in the bidisperse brush.

In Fig. 3a we elaborate on the end-point distribution of the separate fractions in the same bimodal brushes already discussed in Fig. 2. As could be anticipated from the overall profiles, with increasing length difference of the two fractions, we observe a clear increase in the segregation of chain ends. A difference of 20 segments ($N_1 = 90$ and $N_2 = 110$) is enough to reduce the volume fraction of end points of the long fraction to almost zero close to grafting interface. As expected the segregation is strongest for the largest difference in length. Indeed, the region where one finds many end points of the short chains is depleted with the end points of larger ones. The inverse is true of course as well, but this is less of a surprise. Clearly the fluctuations of end points of chains of a particular length are strongly suppressed. Below, we will return to this in more detail.

We can use the end-point distribution to evaluate the average stretching of the chain as a whole. This is done by defining the height H_e of the chain by the first moment over the end-point distribution and normalizing this height by the degree of

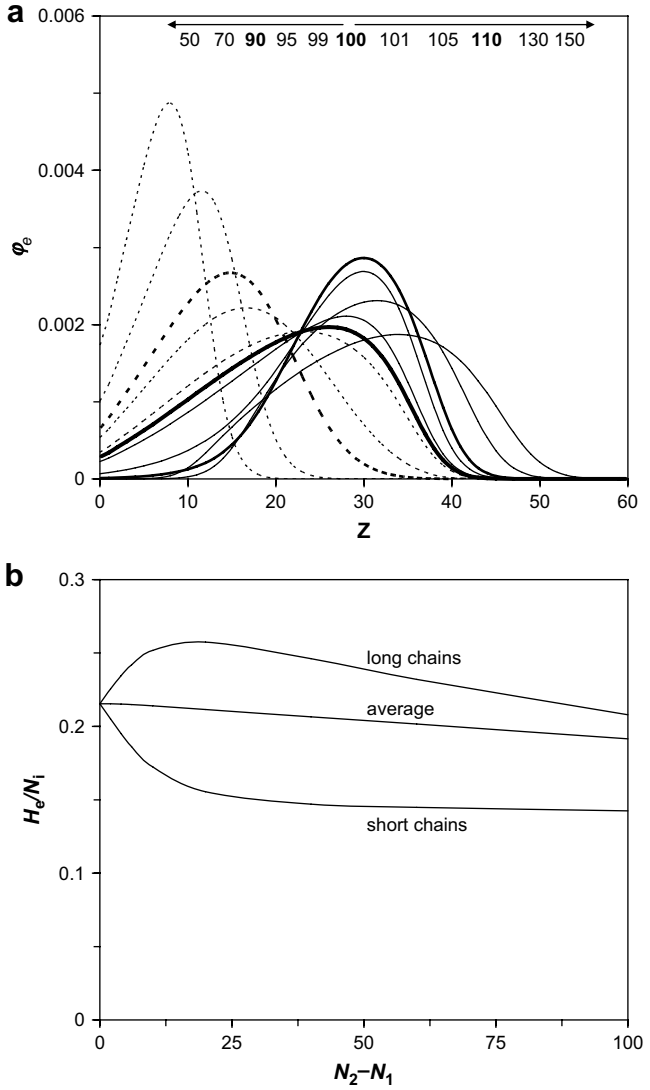

Fig. 3. (a) End-point density profiles $\varphi_e(z)$ of brushes containing two fractions, one fraction increases in length (solid lines) and the other decreases (dotted lines) an equal amount corresponding to the results discussed in Fig. 2. (b) The average height increase per monomer H_e/N_i as a function of the difference between the lengths of the long and short chains. The height is measured as the first moment of the end-point distribution. Curves for the long and the short chains are given as well as the average between these two.

polymerization N_i. The first moment (or average height) of fraction i of component x is given by

$$H_{x,i} = \sum_{z=1}^{z=N_i} z\varphi_{x,i}(z) \Big/ \sum_{z=1}^{z=N_i} \varphi_{x,i}(z) \tag{3}$$

The normalized average stretching H_e/N_i (the average stretching per monomer) is shown in Fig. 3b for both the short and the long fractions. For the long fraction the average stretching increases when going to small length differences and then decreases again for larger length differences. The total average stretching is determined by two parts of the brush, the part in which small chains are present and the part where they are not present. In the first part the chains of the long fraction stretch stronger (this decreases the conformation entropy), to allow more segments in the part of the brush where no short ones are present (increasing the conformation entropy). In the second part the chains of the long fraction stretch less strong as the polymer density in the outer region is relatively low. This causes the maximum in average stretching. The stretching of the short chains, however, decreases monotonically to a plateau value with increasing length differences.

More importantly the average stretching of the chains, which is also plotted in Fig. 3b decreases slightly with increasing size difference. This very clearly points to the driving force for the large changes in the individual profiles. With increasing size difference there is more freedom (compared to a monodisperse brush) to distribute the stretching of the chains as favorable as possible (reducing the entropy losses of the strongly stretched chains). We recall that even though the average stretching is reduced, we find, completely in line with earlier investigations of bimodal brushes [9], that with increasing differences between the long and the short fractions, the height of the brush increases.

3.2. Polydisperse brushes with a realistic size distribution

Predictions for the structure of polymer brushes with an experimentally relevant chain length polydispersity are not found in the literature. This is remarkable as the effects of polydispersity are both large and non-trivial. We will attempt to rationalize the results for polydisperse brushes from the knowledge collected from the analysis of the bidisperse brush.

The first result is, once again, the overall volume fraction profiles of polydisperse brushes. In Fig. 4a we show a set of such graphs for systems with increasing, but still very low, levels of polydispersity. For comparison the homodisperse brush is also presented (most concave, the so-called parabolic profile). As explained in Section 2, we have chosen for the Schulz–Zimm distribution, a size distribution commonly used to describe experimental samples. As can be seen in Fig. 4a, polydispersity has a strong effect on these profiles, even for polydispersities considered low from a synthetic point of view. Upon going from a polydispersity of unity (homodisperse brush) to a polydispersity of $M_w/M_n = 1.1$, the profile changes from a convex to a linear profile. At higher polydispersities the profile becomes completely concave. Furthermore, the height of the brush, as judged from the distance away from the surface where the volume fraction of the polymer units remains above a detection limit, increases significantly with increasing polydispersity. At a polydispersity of 1.1 the height of the brush (defined as the distance where the polymer concentration drops below 1% of the highest achieved density) increases with regard to the homodisperse brush by ~30%. At a polydispersity of 2 the increase is about 120%. This increase in height is depicted in Fig. 5 and is discussed there.

In Fig. 4b we show the overall end-point distributions of the brushes presented in Fig. 4a. As explained above, in a homodisperse

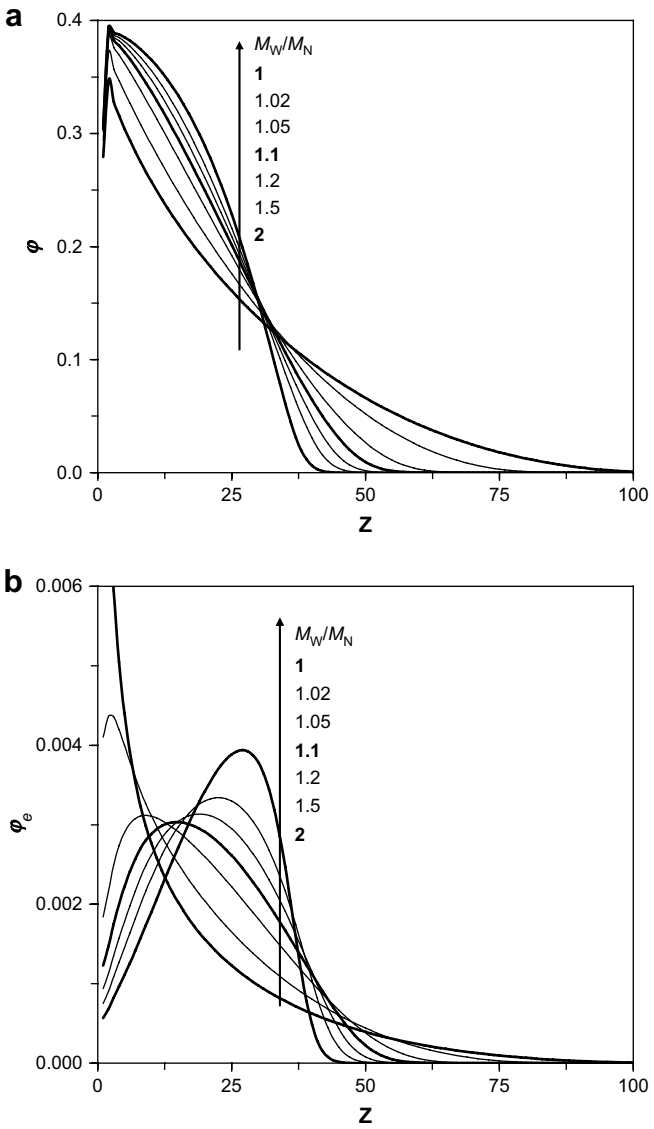

Fig. 4. (a) Overall volume fraction $\varphi(z)$ profile for brushes with increasing polydispersity as indicated. $N_n = 100$, $\sigma = 0.01$, polydispersity with Schulz–Zimm distribution. Cutoff chain length $N_l = 1000$. (b) The corresponding overall distribution of end points $\varphi_e(z)$.

brush there exists a maximum in end-point distribution at the edge of the brush. With increasing polydispersity this maximum moves closer and closer to the grafting interface, even though the overall height of the brush increases. The shift of the maximum of the end-point distribution towards the surface and the gradual growth of the overall brush height are typical polydispersity effects that can be traced to the details of the polymer length distribution. As shown in Fig. 1, the Schulz–Zimm distribution increases the number of small chains and has fewer large chains, with increasing levels of polydispersity. This causes the increase of chains' ends close to the grafting interface. As in the bidisperse brush, we can deduce the average stretching of the chains in the polymer brush by the average positions of the end points. The average height (first moment) of the end points is shown in Fig. 5.

In Fig. 5 the relative height is shown as a function of polydispersity. Here we use three different definitions of the brush height. The first "end" of brush, is defined as the distance where the polymer concentration drops below 1% of the highest achieved density, and is intended to describe the height where the brush

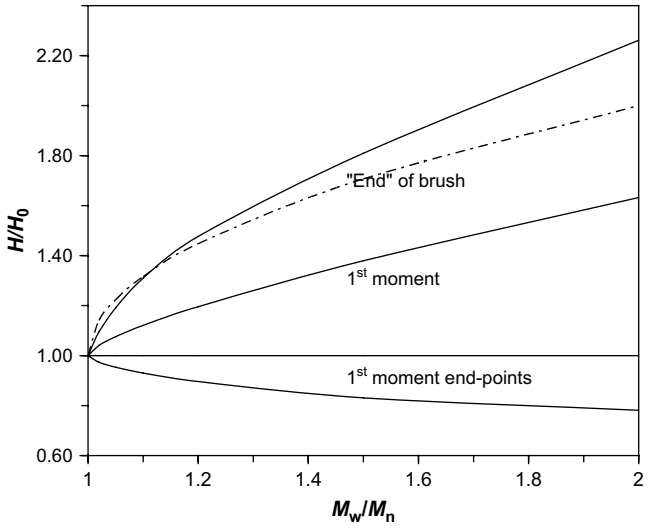

Fig. 5. The height (H) of a brush ($N_n = 100$, $\sigma = 0.01$) relative to the height of a corresponding monodisperse brush (H_0) as a function of polydispersity. The various definitions of the heights are discussed in the text. The dotted line is the prediction for the end of brush by Klushin and Skvortsov [8].

ends. As can be seen, the effect of polydispersity on this is large, the brush height more than doubles when comparing a monodisperse brush with a brush of $M_w/M_n = 2$. However, this definition of the brush height is rather arbitrary, changing the above discussed 1% to a different value, such as 0.1%, has a large effect (the lower this percentage, the stronger the height increases with increasing polydispersity).

The arbitrary choice for the end of brush definition also makes it hard to compare these results to the prediction of Klushin and Skvortsov [8] (see Section 1), even more so as their definition for the end of a brush is different from the one we use. In aSCF theory the end of a brush is defined as the height where the density goes to zero, a well defined point in aSCF theory as only the most probable conformation of a chain is taken into account. In nSCF theory all possible conformations are taken into account which makes it impossible to use the aSCF definition as this would always give the contour length of the longest polymer (there is always a very slight possibility that this chain is completely stretched, thus the density goes to zero at the contour length). Still, we can say that the prediction of Klushin et al. compares well with our (arbitrary) definition. Indeed, the prediction shows a strong increase in height for low polydispersities and a lower more linear increase in height for higher polydispersities, very similar to our calculated end of brush and also similar to our other definition of the height, that is, the first moment over the overall volume fraction profile.

The first moment, or average height (see Eq. (3)), is a far more useful definition of brush height, and is also shown in Fig. 5. Wijmans et al. [17] used this definition of height to compare aSCF and nSCF polymer brush theory. The definition is not arbitrary and has the large advantage that it can be experimentally determined by reflection techniques such a neutron reflection and ellipsometry. This average height of the brush is also strongly influenced by polydispersity. At a polydispersity $M_w/M_n = 1.1$ of the brush height increases 12% compared to a monodisperse brush, at a polydispersity of $M_w/M_n = 2$ the height has increased 60%. Measuring the average height as a function of polydispersity could be a method to prove the huge effects of polydispersity on polymer brushes as demonstrated in this paper.

The final definition of height used in Fig. 5 is the first moment of the end points. As was discussed for the bidisperse brushes, the first moment of end points is directly related to the average stretching. Thus, in Fig. 5 we observe that the average stretching at $M_w/M_n = 1.1$ is 7% lower compared to that of the monodisperse brush. For $M_w/M_n = 2$, the average stretching is even 22% lower. This reduction of stretching was earlier also observed for bimodal brushes as discussed above and can be explained in exactly the same way. With increasing polydispersity there is more freedom (compared to a monodisperse brush) to distribute the stretching of the chains as favorable as possible.

In this paper we only show results for polydispersities up to a value of $M_w/M_n = 2$ as calculated with just a single distribution function (Schulz–Zimm). In a realistic macromolecular system however, the polydispersity might be much higher and/or the distribution function might be different. We have also investigated higher polydispersities (results not shown, up to $M_w/M_n = 10$) and find that the trends reported here for polydispersities between $M_w/M_n = 1$ to $M_w/M_n = 2$ continue. Thus with increasing polydispersity the height of the brush increases while the average stretching decreases. For these high polydispersities the shape of the density profile is similar to the concave profile that was found for $M_w/M_n = 2$ (Fig. 4), the higher the polydispersity the more concave the profile becomes. Furthermore we have also investigated two other distribution functions (Gaussian distribution and uniform distribution). We found for these distributions exactly the same trends as a function of polydispersity as for the Schulz–Zimm distribution although for a given polydispersity there are small differences in the brush density profiles of the different distributions. We believe that the question of the distribution function will become more relevant when good experiments on the effects of polydispersity become available, and can be compared to the model results.

In the above section we predicted a large effect of polydispersity on the height and the density profile of a brush. No experimental evidence exists for these large effects. Indeed, it would be interesting to set up such experiments. Most experimental studies investigating polymer brushes have focused on investigating height as a function of the average degree of polymerization (N_n) and the grafting density (σ) [22,23]. Results have then be compared to the scaling prediction from Alexander and de Gennes (AdG) [24,25]: $H \sim N_n\sigma^{1/3}$. This scaling law was derived from a so-called box model (in which all polymers are assumed to stretch exactly the same amount) but is also found for more sophisticated models like aSCF and nSCF [1,17]. The experimental results were found to be in agreement with this scaling law although polydisperse brushes were used. It is therefore interesting to look at the effect that polydispersity has on the exponents for the AdG scaling law. In Fig. 6 we show the results of the determination of these exponents for different polydispersities. The exponents were determined by fitting the average height of a number of average polymer lengths ($N_n = 100$, 200, 400, 800) and a number of overall grafting densities ($\sigma = 0.05$, 0.1, 0.2, 0.4). As can be seen in Fig. 6, the scaling exponents are almost independent of the polydispersity. This is a surprising finding if we take into account the large effects that polydispersity has on the brush density profile. The scaling exponent for N_n is for all polydispersities slightly lower than the predicted exponent ($\alpha = 1$). We believe this is due to the slight depletion interaction between the polymer and the wall, which slightly increases the average height. As this effect is relatively large for small N_n, the scaling exponent is slightly smaller than 1. The scaling exponent for σ ($\alpha = 1/3$) is almost exactly the same as the predicted exponent. These results compare well to the fact that experimental results in which polydisperse polymer brushes were found to be consistent with scaling exponents as predicted for monodisperse brushes.

3.3. The internal structure of a polydisperse brush with a realistic size distribution

Up till now we have focused on the effect of polydispersity on the brush as a whole. However, as observed with the bidisperse brush, the effects on the internal structure of the brush were even

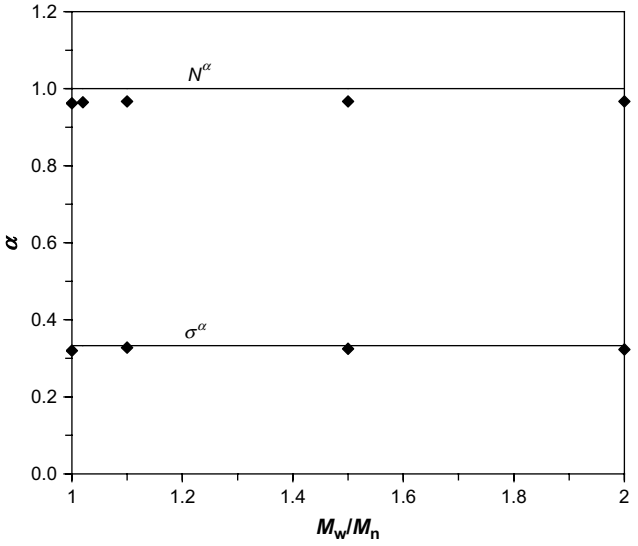

Fig. 6. Brush scaling exponents α for polymer length ($N_n{}^\alpha$) and grafting density (σ^α) as a function of polydispersity. The lines are the theoretical values for the monodisperse brush; the points are calculations.

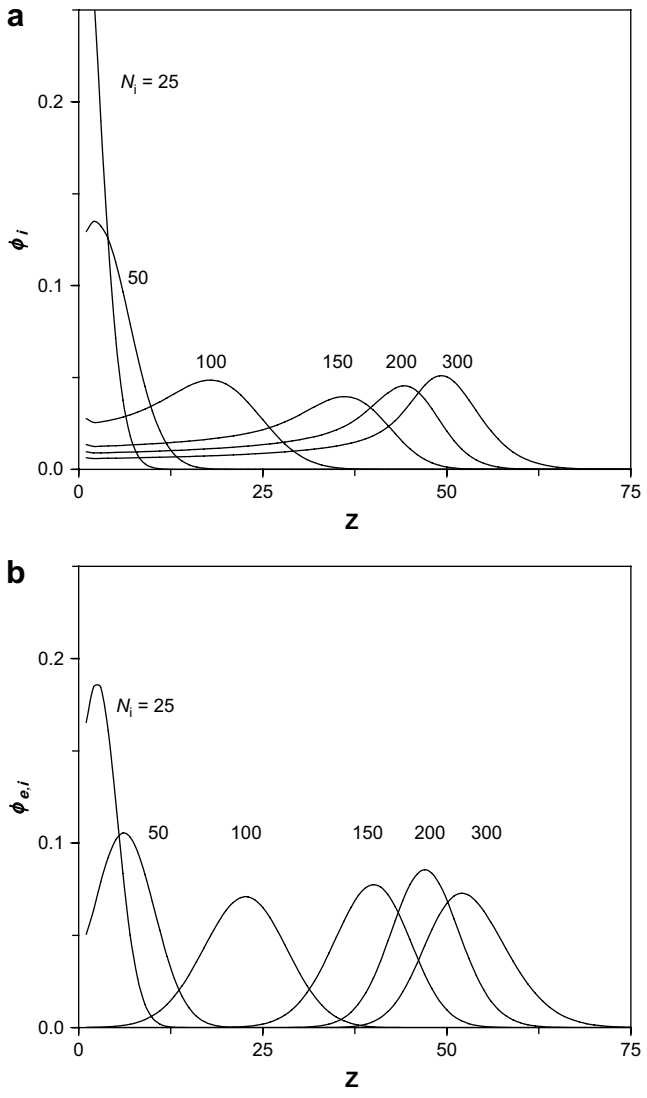

Fig. 7. (a) Normalized brush density profiles, $\phi_i = \varphi_i/\sigma_i N_i$ for a selection of single chain length fractions (N_i as indicated) in a polydisperse ($M_w/M_n = 1.1$) brush. (b) Normalized end-point distribution profiles $\phi_{e,i} = N_n(\varphi_i/\sigma_i N_i)$ for a selection of single chain length fractions (N_i as indicated) in a polydisperse ($M_w/M_n = 1.1$) brush.

more drastic than the changes on the overall density profile. To get similar information for the internal structure of a polydisperse brush, we focus on one case, namely the polydispersity $M_w/M_n = 1.1$. Even for such relatively low degree of polydispersity there is a problem in presenting the data because the grafting density for different chain length fractions is very different. Therefore, the density profiles shown in Fig. 7 have been normalized by $\sigma_i N_i$, the total amount of each fraction, to adjust for these large differences in mass of the different fractions. As a result all the distributions in Fig. 7 have the same integral. As anticipated we observe strong similarities with the effects that were discussed for the bidisperse brush. Again, there is a segregation of the different polymer chains based on length. Of course the shortest chains are located the closest to the surface and the longer ones are further away from the surface. However they do not assume the 'normal' distributions as in the equivalent homopolymer brush cases. Indeed, the short chains appear more compressed and the longer ones assume the characteristic flower-like conformation with a stem (with homogeneous density profile, indicated the strong stretching) and a crown (with increasing density profile, indicating less strong stretching).

In Fig. 7b we show that the end points of different lengths are completely segregated based on chain length. The same normalization is used as in Fig. 7a, however the end-point distributions were also multiplied by N_n to give the same scale as in Fig. 7a. One remarkable observation from Fig. 7b is that the different chain lengths show very similar width of the end-point distribution, indicating that the fluctuations become independent of the chain length. This is a remarkable result especially when we recall the result for the homodisperse brush which features anomalously large fluctuations. Grouping chains of different lengths into "bins" and thus reducing the number of chain fractions to the number of bins has corresponding effects on the fluctuations of end points in each bin. The fluctuations then scale with the bin size. Thus reducing the polydispersity to just one bin (monodisperse case) we retrieve the fluctuations to be of order N.

In Fig. 8 we show the average stretching of the different fractions in a polydisperse polymer brush. Large differences in stretching are found for the different fractions, the fraction with length $N_i = 150$ stretches almost twice as much as the fraction with $N_i = 50$. Long chains tend to have a stronger stretching than short chains up to a certain length. In the brush it is favorable for the longer chains to stretch further and for the short chains to fill this "gap". This has already been observed in a bidisperse brush with two chemical identical polymers of different lengths (see above), the shorter chains are pressed towards the wall, whereas the longer polymers stretch stronger away from the wall. For the longer lengths however, stretching decreases as these chains reach the outer part of the brush where the polymer density is lower. It is also seen that the shortest chains (smaller than $N_i = 40$) have an increased stretching compared to $N_i = 50$. We attribute this to slight depletion interaction between the polymer chain and the wall causing a slightly stronger stretching. This effect is in principle rather small, however, it is large enough to influence the average stretching of these short polymers.

3.4. A box model for polydispersity: a stack of boxes

From the numerical SCF calculations presented above, we have gained detailed insight into the effect of polydispersity on a polymer brush. Polydispersity strongly affects the density

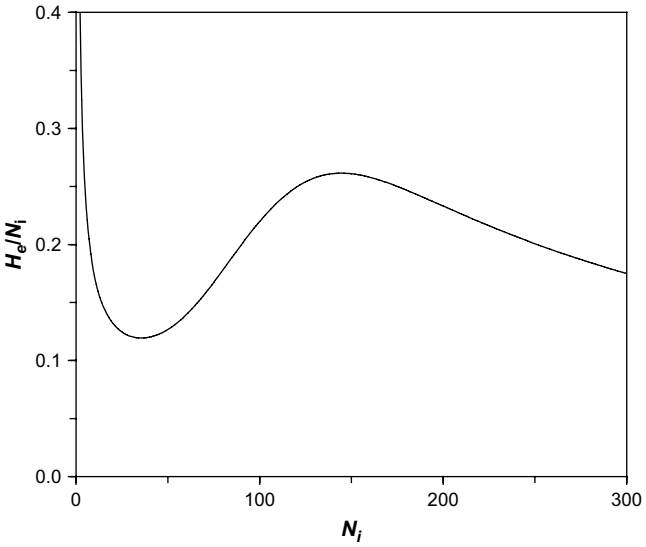

Fig. 8. Average normalized chain stretching H_e/N_i as a function of fraction degree of polymerization.

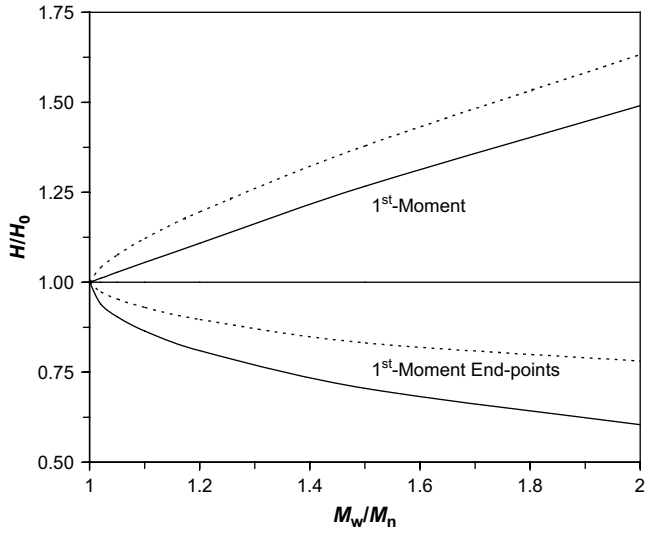

Fig. 10. The height (H), as measured by the first moment over the overall volume fraction (1st moment) and that of the end points (1st moment end points), of a brush ($N_n = 100$, $\sigma = 0.01$) relative to the height of a corresponding monodisperse brush (H_0) as a function of polydispersity. Continuous lines as calculated from the SOB model, dotted lines from nSCF (same as Fig. 5).

profile, the brush height, leads to segregation of end points, but does not affect the scaling exponents of average height with the degree of polymerization and the grafting density. An interesting question is then if one could use some outcomes of our nSCF model as input to create a much simpler model describing the effects of polydispersity. Alexander and de Gennes used a box model [24,25] as a simple description for a polymer brush. In that model all end points are assumed to be in the same plane above the grafting interface and thus all polymers are assumed to stretch exactly the same amount. For the description of a polydisperse brush we propose a stack of boxes (SOB) model. This model is worked out in Appendix 3, but a short explanation is given here.

In the SOB model we assume that all end points of polymers *with the same length* are in the same plane above the grafting interface. However, as we take into account polymers of different lengths we use a stack of boxes, with a number of boxes equal to the number of different chain length fractions. The first box (at the grafting interface) contains all chain length fractions. The second box contains all chain length fractions except the smallest. The third contains all chain length fractions except the smallest two, etc. This continues till the last box which only contains the longest chain length fraction. Thus every box has its own local grafting density determined by the number of chains in all the chain length fractions included in that box. Each box also has a local chain length, which is equal to the length of the smallest chain length fraction in that box minus all the chain lengths of lower boxes. In this way, the sum of all local chain lengths (of all boxes) is the length of the longest fraction. As every box has a local chain length and a local grafting density, we can calculate properties such as its height, its density and its position z for every box. In this model the local chain stretching is *only* determined by the local chain density and we ignore that in reality the local chain stretching is *also* determined by the chain length N. This model is worked out in Appendix 3. The results of this model for the same parameter settings as in Fig. 4 are shown in Fig. 9.

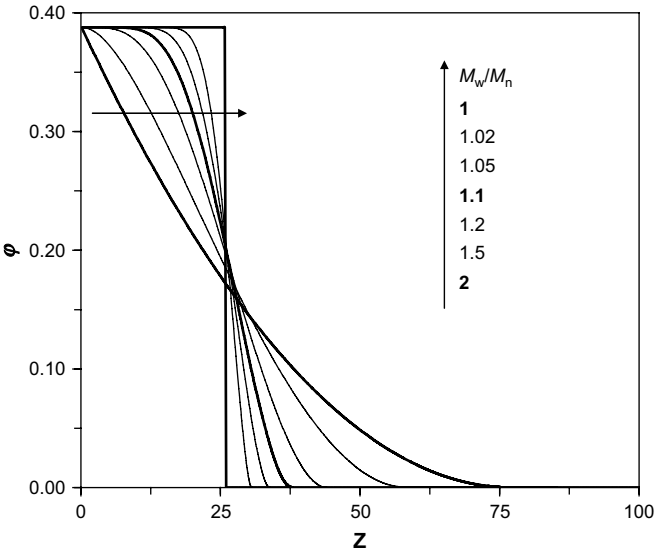

Fig. 9. Overall volume fraction $\varphi(z)$ profile for brushes with increasing polydispersity as indicated as calculated using an SOB model. $N_n = 100$, $\sigma = 0.1$, polydispersity with Schulz–Zimm distribution.

When comparing the results of the stack of boxes model with the results of the nSCF calculations we see that the SOB model gives qualitatively the same results. The density profile shifts with increasing polydispersity from the Box profile, to a more parabolic profile, at higher polydispersity to a more linear decrease and at the highest polydispersity to a completely concave profile, resembling an exponential decrease.

In Fig. 10 we make a more quantitative comparison between the SOB model and the nSCF model, by showing the calculated relative heights as a function of polydispersity. The SOB model predicts, in agreement with the nSCF model, all large increase in first moment, or average height, as a function of polydispersity. However, especially at low polydispersity this relative increase in height is underestimated. An explanation for this is presented in the same picture; the SOB model overestimates the decrease in average stretching, compared to the nSCF model thus leading to a lower average height. As discussed, with increased polydispersity there is more freedom (compared to a monodisperse brush) to distribute the stretching of the chains as favorable as possible. However, in the box model the increase of polydispersity provides the brush with

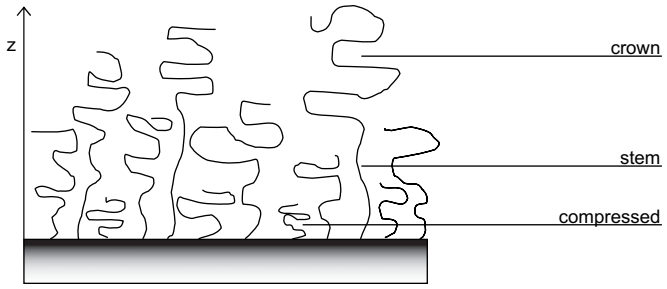

Fig. 11. Schematic representation of stretching in a polydisperse polymer brush. Short chains stretch less than longer chains (compressed). Long chains stretch strongly (stem) when surrounded by smaller chains and decrease their stretching (crown) when only surrounded by longer chains. The longest chains stretch to the end of the brush.

an extra form of freedom, namely the distribution of free ends through the entire brush. In a monodisperse brush, as described by the box model, all free ends are assumed to be in the same plane. With increasing polydispersity the free ends are spread throughout the brush, which leads to a strong reduction in stretching. In the nSCF model, the free ends are already spread throughout the whole brush in the monodisperse case. Therefore the nSCF model shows a much lower reduction is stretching than the SOB model.

The SOB model gives qualitatively the same results as the nSCF model and as such well describes the trends of polydispersity. As box models can be easily extended to investigate particle adsorption in polymer brushes (for example [21]) we believe that the SOB model could well be used to investigate the effect of polydispersity on the adsorption in polymer brushes.

4. Conclusions

A detailed investigation for a polymer brush is given on the effect of polydispersity with a realistic size distribution. The numerical SCF model results show that polydispersity strongly affects the density profile of a brush and that with increasing polydispersity the density profile changes from parabolic to linear to concave, the concave resembling an exponential decrease in density. Also the average height of the brush increases with increasing polydispersity. Going from the monodisperse case to $M_w/M_n = 1.1$ increases the average height by 12%, going to $M_w/M_n = 2$ increases the average height by 60%. We believe that such an effect could well be experimentally determined if one would have corresponding polymer brushes with a significant difference in polydispersity. The average stretching of the brush is found to decrease with increasing polydispersity. With increasing polydispersity there is more freedom (compared to a monodisperse brush) to distribute the stretching of the chains as favorable as possible. Despite these large effects of polydispersity, the exponent with which the average height scales with the grafting density and the degree of polymerization of the brush are unaffected by polydispersity.

The internal structure of the brush is even more radically influenced by polydispersity. A schematic depiction of our proposed structure of a polydisperse brush is given in Fig. 11. There is a segregation of the different polymer chains based on length. Short chains are compressed close to the grafting interface while the longer ones assume a characteristic flower-like conformation with a stem (strong stretching) when surrounded by smaller chains and a crown (less strong stretching) when surrounded by longer chains. The longest chains have the same conformation with the stem when surrounded by smaller chains and the crown at the end of the brush. The end points of different lengths are completely segregated based on chain length. Different chain lengths show very similar end-point fluctuations, indicating that the fluctuations become independent of the chain length. This is a remarkable result especially when we recall the result for the homodisperse brush which features anomalously large fluctuations. The chains in the polydisperse brush have anomalously small fluctuations.

Most of the effects observed for polydisperse brushes can also be observed and understood when looking at the simplest form of polydispersity: bidispersity. With increased bidispersity we also observe an increase in average height, a decrease in average stretching and the compression of the short chain fraction and the flower-like distribution for the long chain fraction.

The results of a much simpler model based on the well-known concept of the box model compare well to the nSCF model, although the reduced average stretching as a function of increased polydispersity is somewhat overestimated. This model, in which we describe a polydisperse brush as a stack of boxes, might prove useful when investigating the uptake of particles in a polydisperse brush.

Acknowledgements

We thank P.M. Biesheuvel for the interesting discussions leading to the start of this project and we thank Unilever Research, Port Sunlight, UK, for encouragement and funding.

Appendix 1. The SF-SCF formalism for end-grafted polydisperse polymer systems

Here we follow the approach of Roefs et al. [16]. Polymer chains of type $i = 1, \ldots, I$ have a degree of polymerization N_i, ranked in increasing values of the chain lengths. This means that N_I is the largest one. For simplicity we will assume that chain i has a degree of polymerization equal to the chain ranking number, i.e. $N_i = i$, so that there exists one normalization per length. For given polydispersity the probability P_i of a chain i is known. Let the overall grafting density be given by σ, then the grafting density of a chain of type i is given by $\sigma_i = P_i\sigma$. Each chain has segment ranking numbers $s = 1, \ldots, N_i$, where it is understood that segment $s = 1$ is positioned at the first non-grafted segment just next to the surface, i.e. at $z = 1$. Here we assume that all polymers are composed of the same segment type and that just one segment potential exists, given by $u(z)$. This segment potential is used in the Boltzmann weight $G(z) = \exp - u(z)/k_BT$. We split up the formalism in a forward and a backward propagator. The forward starts with segment number 1 with the end-point distribution $G(z,1) = G(z)\delta(z,1)$, where $\delta(z,1) = 1$ when $z = 1$ and zero otherwise. The recurrence relation reads for a 6-choice cubic lattice

$$\begin{aligned} G(z,s) &= G(z)[G(z-1,s-1) + 4G(z,s-1) + G(z+1,s-1)]/6 \\ &= G(z)\langle G(z,s-1)\rangle \end{aligned} \tag{A1}$$

which defines the angular brackets as a three layer average. Eq. (A1) is performed for each coordinate z and all segments up to $s = N_I$. Let us, for purposes of normalization obtain the single chain partition function Q_i for chain i:

$$Q_i = \sum_{z=1}^{N_i} G(z, N_i) \tag{A2}$$

Using this single chain partition function we can find the normalization C_i for chain i:

$$C_i = \frac{\sigma_i}{Q_i} \tag{A3}$$

It is understood that when a particular chain length j is absent $C_j = 0$.

From Eqs. (A1) and (A3) we now can already identify the volume fraction profile of all chain ends, which we denote by $\varphi_{e,i}(z)$:

$$\varphi_{e,i}(z) = C_i G_i(z,i) \tag{A4}$$

To evaluate also the distribution of the other segments we need a backward propagator. This propagator is somewhat more complicated because we are going to add contributions for all chain lengths in this operation together. For this the end-point distribution $G(z,s|N \geq s)$ is introduced, which is the total statistical weight of all conformations that start with free end and arrive at segment s at coordinate z. Obviously, only the chains that are longer or equal than s can contribute to this end-point distribution and this is expressed behind the vertical bar. We start the propagator by the end of the longest chains, i.e. $s = N_l$ and write $G(z,N_l|N \geq N_l) = C_{N_l} G(z)$ for all z (there is no constraint). The backward equivalent of Eq. (A1) is

$$G(z,s|N \geq s) = G(z)\langle G(z,s+1|N \geq s+1)\rangle + C_N G(z) \tag{A5}$$

which is performed N_l times. The overall volume fraction profile is now easily computed by

$$\varphi(z) = \sum_{s=1}^{N_l} \frac{G(z,s|N \geq s)G(z,s)}{G(z)} \tag{A6}$$

To compute volume fraction profiles for a sub-fraction of the chains one can use the classical method by computing the volume fraction of each chain length separately.

Appendix 2. Local chain stretching

In analytical brush theory for monodisperse brushes, as developed by Zhulina et al. [26] and Milner et al. [27], local chain stretching plays an important role. This is exemplified in the analytical description for the free energy of a polymer brush [17]

$$\frac{A}{LkT} = \frac{3}{2b^3}\int_0^H \mathrm{d}z'\varphi_e(z',N)\int_0^{z'} \mathrm{d}z E(z,z',N) + \frac{1}{b}\int_0^H f[\varphi(z)]\mathrm{d}z \tag{A7}$$

Here A/kT is the dimensionless free energy, L is the total surface area, b is the segment size (equal to the lattice spacing). The second term of this equation accounts for the free energy of mixing of the grafted chains with other molecules in the system. $f[\varphi(z)]$ being the free energy density of mixing, which depends on $\varphi(z)$. However, we focus on the first term of this equation, which represents the contribution from the elastic chain stretching in the brush layer. In this term $E(z,z',N)$ gives the local stretching of a chain at a give distance from the grafting interface z and for a give position of the end point z' ($z' > z$). Thus the stretching function $E(z,z',N)$ determines the position of every segment for a given end-point position. For homodisperse brushes the stretching function is given by

$$E(z,z',N) = \frac{\pi}{2N}\left(z'^2 - z^2\right)^{1/2} \tag{A8}$$

As can be seen, this function leads to a parabolic profile. When depicting this stretching function, it is convenient to plot $E(z,z',N)^2$ as a function of z^2.

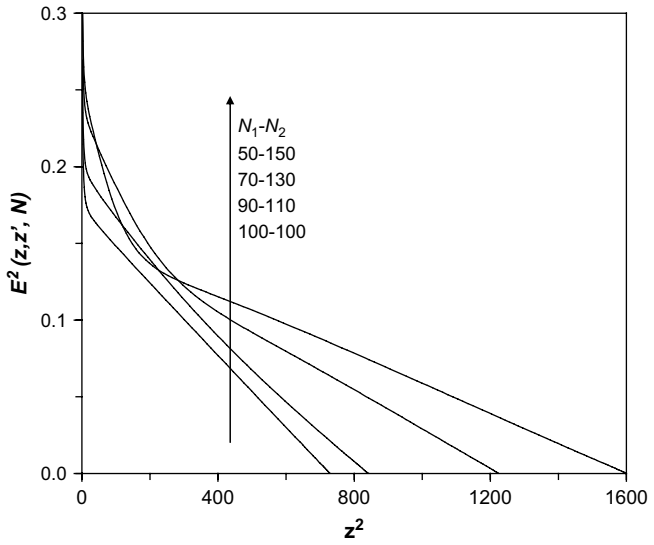

Fig. 12. The squared local chain stretching for a given end-point position $E^2(z,z',N)$ for the long chain in bidisperse polymer brushes as described in Fig. 2 as a function of the squared distance.

The local stretching can also be determined in numerical SCF calculations. For this we rank the chain segments $s = 1,\ldots, N_i$, where segment $s = 1$ is positioned at the first non-grafted segment just next to the surface, i.e. at $z = 1$. We then calculate the density profile for a given rank number and given end-point position and chain fraction $\varphi_i(z,s|z',N_i)$. From this we can calculate the first moment (or average height) of the given segment s

$$\langle z\rangle_s = \sum_{z=1}^{z=N_i} z\varphi_i(z,s|z',N_i) \Big/ \sum_{z=1}^{z=N_i} \varphi_i(z,s|z',N_i) \tag{A9}$$

For given z' and N_i, we can plot $\langle z\rangle_s$ as a function of s, and compute $\delta\langle z\rangle_s/\delta s$ and thus

$$E(z,z',N_i) = E(\langle z\rangle_s,z',N_i) = \left.\frac{\delta\langle z\rangle_s}{\delta s}\right|_{\langle z\rangle_s} = \left.\frac{\langle z\rangle_s - \langle z\rangle_{s-1}}{1}\right|_{\langle z\rangle_s} \tag{A10}$$

In Fig. 12 we show the squared stretching function as determined by nSCF for a monodisperse brush and three corresponding bidisperse brushes. As can be seen, the squared local stretching for a monodisperse brush indeed gives a linear profile (except close to the wall due to the small depletion interaction between the grafting interface and the polymer chains). Extrapolating this linear profile to $z = 0$ gives a squared local stretching of 0.18, identical to what one can calculate from the analytical equation (Eq. (A8)) ($N = 100$, $z' = 27$).

For bidisperse brushes the squared local chain stretching (of the long chain fraction) shows a linear dependence until at a certain z the slope changes. The distance z where the kink is observed depends on the length of the small chain fraction; the longer the small chain fraction the further away the kink is. The larger the difference between the long and the short chain, the more pronounced the kink is. The observation that the squared stretching function of the long chain in a polydisperse brush consists of two linear parts with different slopes could be very useful when developing analytical theory for bi- and polydisperse brushes.

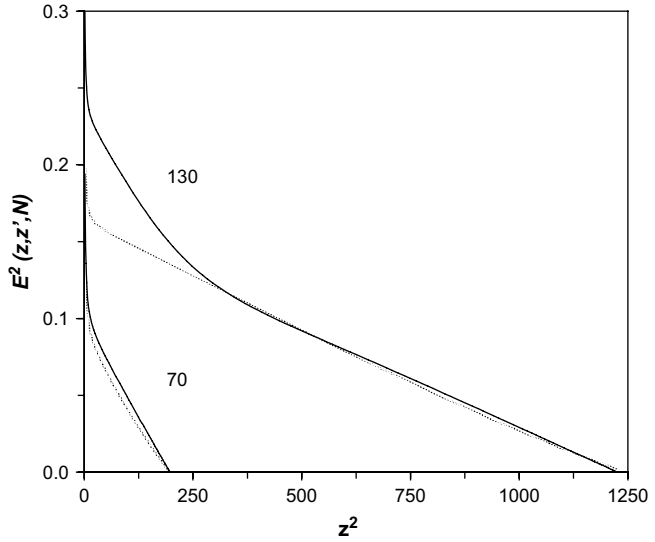

Fig. 13. The squared local chain stretching for a given end-point position $E^2(z,z',N)$ as a function of the squared distance, for a long and a short chain ($N_1 = 70$, $N_2 = 130$) in a bidisperse brush ($\sigma_1 = \sigma_2 = 0.05$, continuous lines) and corresponding monodisperse brushes ($N = 70$, $\sigma = 0.1$ and $N = 130$, $\sigma = 0.05$, dotted lines).

In Fig. 13, the local chain stretching of a long and a short chain in the same bidisperse brush is compared. This shows very clearly that close to the grafting interface the long polymer is stretched much more strongly than the short polymer. At $z = 7$, the local chain stretching of the long chains is twice that of the short chains. The squared local stretching of the short chain follows a linear profile as such its density profile will be parabolic. There is only a slight difference between the local stretching of the short chain in the bidisperse brush and a corresponding monodisperse brush (dotted line). This is unexpected as in Fig. 2b we have seen that the short chain fraction becomes more compressed. This stretching function, however, is only for all chains with a given end-point position $z = 14$, which is close to the end of the short chain fraction density profile. In the bidisperse brush most short chains are compressed, however the few who stretch to $z = 14$ stretch somewhat more than they would in a monodisperse brush. Due to the compression of other chains they are somewhat pushed out of the area with a higher chain density leading to a slight increase in stretching. When we compare the squared local stretching of the long chain in the bidisperse brush with the squared local stretching of its corresponding monodisperse brush, there is a large difference when the long chain is surrounded by short chains in the bidisperse brush, above the short chain fraction the stretching functions are very similar.

Appendix 3. A quasi-analytical box model for the polydisperse polymer brush: the stack of boxes model

The simplest model for a homodisperse polymer brush is one in which one assumes that all the polymers in the brush have the same stretching and thus that all end points are at the same distance from the grafting interface. This so-called box model was first used by Alexander and de Gennes [24,25] and yielded for uncharged polymers brushes to simple scaling laws for, e.g. the brush height. Using a Gaussian model, one can write a free energy $F(H) = E - TS$ as being composed interaction part $E \sim v\sigma N^2/H$, where v is the second virial coefficient (which is unity in good solvent, and will be omitted here), and a loss of entropy $-TS \sim H/N^2$ that originates from the (homogeneous) stretching of the chains. Optimization of the free energy with respect to the height H gives the well-known result

$$H \sim N\sigma^{1/3} \tag{A11}$$

Although the assumption of equal stretching of all polymers is a serious oversimplifications, the same scaling law was also found for more sophisticated models like aSCF and nSCF [1,17]. Advantages of using box models are that they are simple and can easily be extended, e.g. to investigate adsorption in polymer brushes [21].

A polydisperse brush cannot be described by a model that uses just one single box, as one would need to assume that polymers of different length stretch to the same height, and thus that short chains are extremely extended and long ones are then compressed. One can however describe a polydisperse brush by a stack of boxes. One simplistic generalization is found when there are as many boxes as there are chain length fractions. The first box (at the grafting interface) contains all chain length fractions. The second box contains all chain length fractions except the smallest. The third contains all chain length fractions except the smallest two, etc. This continues till the last box which only contains the longest chain length fraction. Thus every box has its own local grafting density determined by the number of chains in all the chain length fractions included in that box. Each box also has a local chain length, which is equal to the length of the smallest chain length fraction in that box minus all the chain lengths of lower boxes. In this way, the sum of all local chain lengths (of all boxes) is the length of the longest fraction. As every box has a local chain length and a local grafting density, we can calculate for every box its height by implementation of Eq. (A11). If every chain length fraction has a width of one monomer (and thus all boxes have a local chain length of one) the height of the total brush is then given by

$$H \sim \sum_{N=1}^{N_l} \left(\sigma - \sum_{i=1}^{N} \sigma_i \right)^{1/3} \tag{A12}$$

In this approach we thus assume that all polymers of the same length stretch exactly the same amount and that the local stretching of a single polymer is only determined by local polymer volume fraction and not by the stretching of the remainder of the chain. Note that these assumptions are very similar to the assumptions made by MWC and BZ [5,6] as they assume complete segregation of end points. For a system with many different polymer lengths, this assumption leads to extremely narrow distributions of end points of polymers with the same height and thus almost the same stretching. Also, MWC and BZ take the point of view that the stretching of the fraction of small polymers is not influenced by the large ones, i.e. that the local stretching is only determined by the local volume fraction. From Eq. (A12), it is possible to extract the local polymer volume fraction by dividing the local "grafting density" by the local height increment. Results of the model are shown in Figs. 9 and 10.

References

[1] Currie EPK, Norde W, Cohen Stuart MA. Adv Colloid Interface Sci 2003;100–102:205.
[2] Zhao B, Brittain WJ. Prog Polym Sci 2000;25:677.
[3] Birschtein TM, Amoskov VM. Polym Sci Ser C 2000;42:172.
[4] Milner ST. Science 1991;251:905.
[5] Milner ST, Witten TA, Cates ME. Macromolecules 1989;22:853.
[6] Birschtein TM, Liatskaya YV, Zhulina EB. Polymer 1990;31:2185.
[7] Lai P-K, Zhulina EB. Macromolecules 1992;25:5201.
[8] Klushin LI, Skvortsov AM. Macromolecules 1992;25:3443.
[9] Dan N, Tirrell M. Macromolecules 1993;26:6467.
[10] Currie EPK, Wagenmaker M, Cohen Stuart MA, Well AAv. Physica B 2000;283:17.
[11] Karim A, Satija SK, Douglas JF, Ankner JF, Fetters LJ. Phys Rev Lett 1994;73:3407.
[12] Kritikos G, Terzis AF. Polymer 2005;46:8355.
[13] Terzis AF, Theodorou DN, Stroeks A. Macromolecules 2000;33:1385.
[14] Edwards SF. Proc Phys Soc 1965;85:613.
[15] Scheutjens JMHM, Fleer GJ. J Phys Chem 1979;83:1619.

[16] Roefs SPFM, Scheutjens JMHM, Leermakers FAM. Macromolecules 1994; 27:4810.
[17] Wijmans CM, Scheutjens JMHM, Zhulina EB. Macromolecules 1992;25: 2657.
[18] Schulz GV. Z Phys Chem 1939;B43.
[19] Zimm BH. J Chem Phys 1948;16:1099.
[20] Terzis AF. Polymer 2002;43:2435.
[21] Biesheuvel PM, Wittemann A. J Phys Chem B 2005;109:4209.
[22] Currie EPK, Leermakers FAM, Cohen Stuart MA, Fleer GJ. Macromolecules 1999;32:487.
[23] Bianco-Peled H, Dori Y, Schneider J, Sung L-P, Satija S, Tirell M. Langmuir 2001; 17:6931.
[24] Alexander S. J Phys (Paris) 1977;38:983.
[25] de Gennes PG. Macromolecules 1980;13:1069.
[26] Zhulina EB, Priamitsyn VA, Borisov OV. Polym Sci USSR 1989;31:205.
[27] Milner ST, Witten TA, Cates ME. Macromolecules 1988;21:2610.